PROCEEDINGS OF SCIENCE

ϕ spin alignment with respect to global angular momentum reconstructed with the 1st-order event plane

Chensheng Zhou for the STAR Collaboration*
Shanghai Institute of Applied Physics & Brookhaven National Laboratory
E-mail: xanthus@rcf.rhic.bnl.gov

The spin alignment of the ϕ-meson is sensitive to different hadronization scenarios and the vorticity of the colliding system. We present the STAR's measurement of spin alignment for ϕ-mesons produced at mid-rapidity with transverse momentum up to 5 GeV/c. The alignment is quantified by the diagonal spin density matrix elements ρ_{00} with respect to the normal of the 1st order event plane, which is reconstructed with the Zero Degree Calorimeters. The results are presented as a function of the transverse momentum and collision centrality for the beam energies of 11.5, 19.6, 27, 39 and 200 GeV. The implications of our results are discussed.

Critical Point and Onset of Deconfinement - CPOD2017
7-11 August, 2017
The Wang Center, Stony Brook University, Stony Brook, NY

*Speaker.

PoS(CPOD2017)048

1. Introduction

Measurements of the particle polarization in relativistic heavy-ion collisions can provide information about the dynamics of the Quark Gluon Plasma (QGP) [1–4]. In particular, the initial global angular momentum in non-central heavy-ion collisions may be transferred by baryon stopping, in part, to the fireball, and lead to the global polarization of produced quarks [5–10]. Through the hadronization process, the global polarization of quarks will be manifested as the global polarization of hyperons as well as the spin alignment of vector mesons. For example, it has been argued [6] that the transverse dependence of the spin alignment of ϕ-meson is sensitive to different hadronization scenarios and the vorticity of the colliding system.

With data taken in year 2004 at the Relativistic Heavy Ion Collider (RHIC), the STAR experiment has published the global spin alignment of $\phi(1020)$ and $K^{*0}(892)$ mesons in Au+Au collisions at $\sqrt{s_{NN}} = 200$ GeV [11]. The study was based on 20 M events and no significant result was reported due to limited statistics at that time. In this analysis, we report STAR's measurement of ϕ-meson spin alignment with respect to the global angular momntum reconstructed with the 1st-order and 2nd-order event planes, with larger data sets taken in year 2010 (100M Au+Au events at $\sqrt{s_{NN}} = 39$ GeV, 3M at $\sqrt{s_{NN}} = 11.5$ GeV) and 2011 (500M at $\sqrt{s_{NN}} = 200$ GeV, 30M at $\sqrt{s_{NN}} = 27$ GeV, 10M at $\sqrt{s_{NN}} = 19.6$ GeV).

For spin-1 vector mesons like ϕ, the spin alignment can be described by a 3×3 spin density matrix ρ with unit trace [12]. The deviation of the diagonal elements of ρ_{mm} $(m = -1, 0, 1)$ from $1/3$ signals about nets spin alignment. Out of three diagonal elements, only ρ_{00} is independent of the other two (ρ_{-1-1} and ρ_{11} are degenerate). For a two-body decay ($\phi \to K^+ + K^-$ in our case), the angular distribution of one of the decay products can be written as:

$$\frac{\mathrm{d}N}{\mathrm{d}(\cos\theta^*)} \propto (1-\rho_{00}) + (3\rho_{00}-1)\cos^2\theta^*, \tag{1.1}$$

where θ^* is the angle between the quantization axis (L) and the momentum direction of a daughter particle (K^+ in this case) in the rest frame of the parent vector meson. Here L is the direction of global angular momentum and is perpendicular to the reaction plane [13]. Fitting the measured $\cos\theta^*$ distribution with the above equation will allow one to extract ρ_{00}.

Possible hadronization scenarios of spin-1 vector mesons have been discussed in [6]. Based on model calculations, the recombination of polarized quarks and anti-quarks in QGP, which likely dominates at low p_T and middle rapidity region, will result in $\rho_{00} < 1/3$, while the fragmentation of polarized quarks, which likely happens at large p_T and forward rapidity region, will result in $\rho_{00} > 1/3$.

2. Data sets and analysis cuts

In our analysis, all data are taken by a minimum bias trigger. ϕ-mesons are reconstructed via the $\phi \to K^+K^-$ channel. Two daughter tracks are required to have more than 15 space points in the Time Projection Chamber (TPC) [14], and their distances of closest approach (DCA) less than 2 cm from the primary vertex. Low-momentum ($p_T < 0.65\,\mathrm{GeV}/c$) K^+ and K^- are identified either by the energy loss ($\langle \mathrm{d}E/\mathrm{d}x\rangle$) inside the TPC, or together with the mass square (m^2) measured by the Time-of-Flight (TOF) detector [15]. At larger momenta ($p_T > 0.65\,\mathrm{GeV}/c$), both the $\langle \mathrm{d}E/\mathrm{d}x \rangle$ and the m^2 information are used for particle identification.

The 1st-order event plane is reconstructed by the Shower Maximum Detector at the Zero Degree Calorimeters (ZDC-SMD) [16] and flattened by the shifting method [13]. The flattening is applied once every 10 runs (about 6×10^4 events in Au+Au collisions at 200 GeV). The 2nd-order event plane is reconstructed by tracks inside TPC.

3. Results and discussions

In our analysis, we obtain the yield of ϕ-mesons by fitting the invariant mass distribution of K^+K^- pairs. The background is obtained using the event mixing technique. Figure 1 shows a typical K^+K^- distribution in the ϕ-meson mass region, which, after background subtraction, is fitted with Briet-Wigner function:

$$BW(m_{inv}) = \frac{1}{2\pi} \frac{A\Gamma}{(m_{inv} - m_\phi)^2 + (\Gamma/2)^2}, \tag{3.1}$$

with the 2nd-order polynomial function for residual background to extract the raw ϕ-meson yield. Here Γ is the width of the distribution. A is the area of the distribution, which equals to the raw yield scaled by the bin width (= 0.001 GeV/c^2).

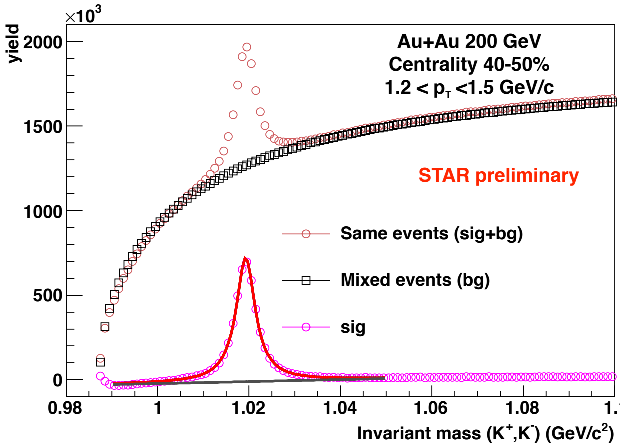

Figure 1: The K^+K^- invariant mass distribution in the ϕ-meson mass region and the corresponding fitting for the centrality class of $40\% - 50\%$, with selection on ϕ-particle's p_T of $1.2 < p_T < 1.8$ GeV/c. The ρ_{00} was estimated from the fit to the data (line).

With the yield of ϕ-particle obtained for different $\cos\theta^*$ bins, we can extract the observed ρ_{00} by fitting the yield distribution with equation 1.1, as shown in Figure 2. The observed ρ_{00} needs to be corrected for finite event plane resolution. The correction factor on $(\rho_{00} - \frac{1}{3})$ is $(\frac{4}{1+3R})$, where $R = \langle \cos 2(\psi_{\text{observed}} - \psi_{\text{real}}) \rangle$ is the event plane resolution which can be determined by the correlation between two sub-events [13].

Figure 3 shows our measurement of ρ_{00} as a function of transverse momentum for Au+Au collisions at $\sqrt{s_{NN}} = 200$ GeV. Non-trivial p_T dependence is seen in this plot. At $p_T \sim 1.5$ GeV/c,

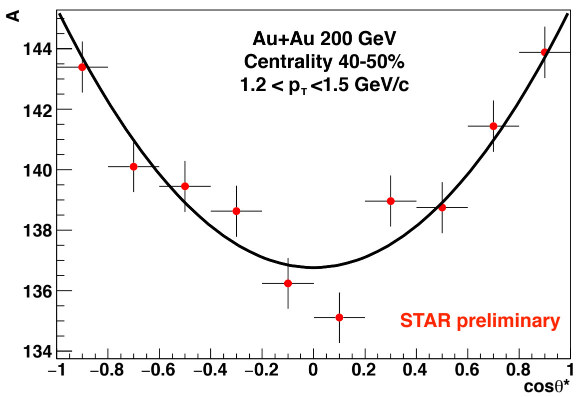

Figure 2: The $\cos\theta^*$ distribution measured for 40%–50% central Au+Au collisions with selection on ϕ-particle's p_T of $1.2 < p_T < 1.8$ GeV/c.

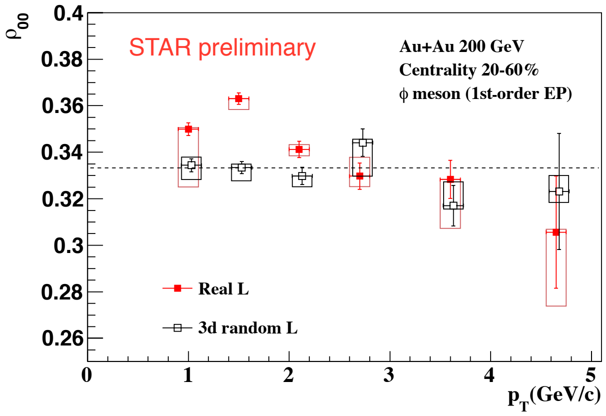

Figure 3: ρ_{00} as a function of p_T for Au+Au collisions at $\sqrt{s_{NN}} = 200$ GeV.

ρ_{00} after event plane resolution correction is significantly larger than 1/3. However, the fragmentation is not expected to dominate the production in this p_T region ($\sim$ 1.5 GeV/c), so the possible reason for the large ρ_{00} requires further theoretical consideration. As a test, the values of ρ_{00} were extracted after randomizing the direction of the quantization axis, L. Values of 1/3 were obtained as expected.

To compare with the result reconstructed with the 2nd-order event plane, we need to take the decorrelation between the 1st- and 2nd-order event planes into considerration:

$$\rho_{00}^{\text{2nd}} - \frac{1}{3} = \frac{1+3D_{12}R_1}{1+3R_2}(\rho_{00}^{\text{1st}} - \frac{1}{3}), \tag{3.2}$$

where $R_{1,2} = \langle \cos 2(\psi_{1,2} - \psi_{\text{real}}) \rangle$ are the event plane resolution for 1st(2nd)-order event plane ($\psi_{1,2}$), and $D_{12} = \langle \cos 2(\psi_1 - \psi_2) \rangle$. Figure 4 shows that, with decorrelation taken into account, the result obtained with the 1st- and 2nd-order event plane are compatible.

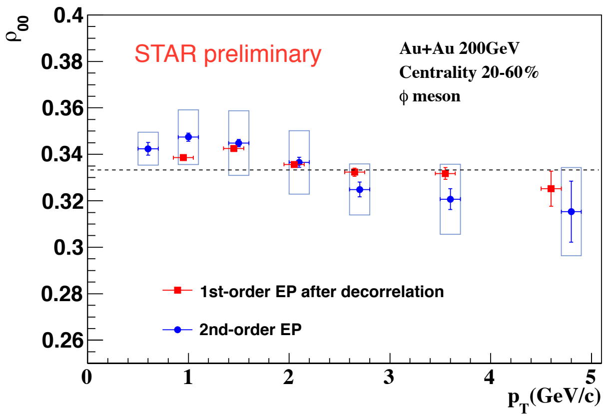

Figure 4: ρ_{00} as a function of p_T for Au+Au collisions at $\sqrt{s_{NN}} = 200$ GeV. In order to compare with the result obtained with the 2nd-order event plane (presented as a poster by X. Sun at Quark Matter 2017, the error was overestimate due to not fully understanding the effect of resolution correction.), the decorrelation formula is used on the result obtained with the 1st-order event plane.

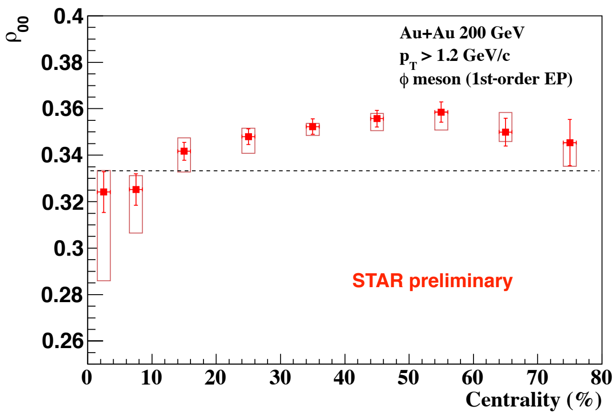

Figure 5: The ρ_{00} as a function of centrality for Au+Au collisions at $\sqrt{s_{NN}} = 200$ GeV.

Figure 5 shows our measurement of ρ_{00} as a function of centrality for Au+Au collisions at $\sqrt{s_{NN}} = 200$ GeV. The upper and lower bounds of the systematic uncertainties in this plot (as well as other plots in this paper) are determined by repeating the study with the combination of different track quality cuts and fitting functions. The result was obtained by integrating the $\rho_{00}(p_T)$ over $p_T > 1.2$ GeV/c to avoid the large systematics associated with the lowest p_T point in Fig. 3. ρ_{00} is around 1/3 in most-central collisions, which is consistent with the small initial angular momentum due to the symmetry. For mid-central collisions, the ρ_{00} is significantly larger than 1/3. The ρ_{00} goes back to around 1/3 in very peripheral collisions, and a possible explanation is that the large initial orbital angular momentum is mostly carried away by spectators and little remains in particles produced at middle rapidity.

In very peripheral collisions when two colliding nuclei just graze each other, although the ini-

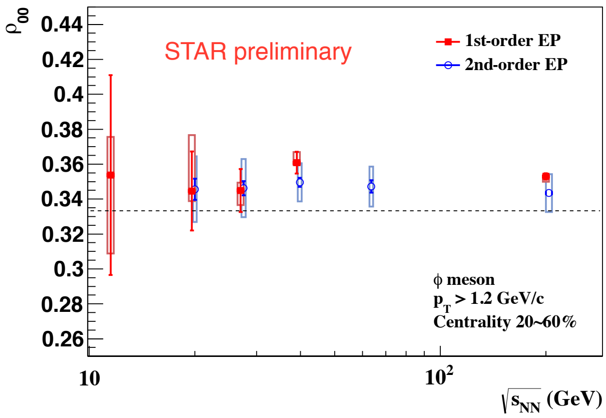

Figure 6: The ρ_{00} as a function of energy for Au+Au collisions.

tial orbital angular momentum is large it is mostly carried away by spectators, and little remains in particles produced at midrapidity; to the other extend, in very central collisions, the initial angular momentum is small due to the symmetry reason.

Figure 6 shows our measurement of ρ_{00} as a function of energy for Au+Au collisions. We observe that ρ_{00} are significantly larger than 1/3 at $\sqrt{s_{NN}} = 39$ and 200 GeV.

4. Summary

Non-trivial dependence of ρ_{00} as a function of p_T and centrality has been observed with the 1st-order event plane for Au+Au collisions at $\sqrt{s_{NN}} = 200$ GeV. The measured ρ_{00} is $> 1/3$ for $1.2 < p_T < 1.5$ GeV/c in non-central collisions. For ρ_{00} integrated from $p_T > 1.2$ GeV/c, the deviation from 1/3 is found to be significant at $\sqrt{s_{NN}} = 39$ and 200 GeV.

This is the first observation of the spin alignment observable, ρ_{00}, deviating significantly from 1/3. Vorticity induced by initial global angular momentum and particle production from quark fragmentation are possible contributions to these observations.

5. Acknowledgments

This work is supported in part by the National Natural Science Foundation of China under Contracts Nos.11421505 and 11220101005, the Major State Basic Research Development Program in China under Contracts No. 2014CB845401, and the Key Research Program of Frontier Sciences of CAS under Grant No.QYZDJSSW-SLH002.

References

[1] P. Hoyer, Phys. Lett. B **187**, 162 (1987).

[2] R. Stock *et al.*, in *Proceedings of the Conference on Quark Matter Formation and Heavy-Ion Collisions*, edited by M. Jacobs and H. Satz (World Scientific, Singapore, 1982).

[3] A. D. Panagiotou, Phys. Rev. C **33**, 1999 (1986).

[4] M. Jacob and J. Rafelski, Phys. Lett. B **190**, 173 (1987).

[5] Z. T. Liang and X. N. Wang, Phys. Rev. Lett. **94**, 102301 (2005) Erratum: [Phys. Rev. Lett. **96**, 039901 (2006)]

[6] Z. T. Liang and X. N. Wang, Phys. Lett. B **629**, 20 (2005) [nucl-th/0411101].

[7] Z. T. Liang, J. Phys. G **34**, S323 (2007)

[8] B. Betz, M. Gyulassy and G. Torrieri, Phys. Rev. C **76**, 044901 (2007)

[9] J. H. Gao, S. W. Chen, W. t. Deng, Z. T. Liang, Q. Wang and X. N. Wang, Phys. Rev. C **77**, 044902 (2008)

[10] F. Becattini, L. Csernai and D. J. Wang, Phys. Rev. C **88**, no. 3, 034905 (2013) Erratum: [Phys. Rev. C **93**, no. 6, 069901 (2016)]

[11] B. I. Abelev *et al.* [STAR Collaboration], Phys. Rev. C **77**, 061902 (2008) [arXiv:0801.1729 [nucl-ex]].

[12] K. Schilling, P. Seyboth and G. E. Wolf, Nucl. Phys. B **15**, 397 (1970) Erratum: [Nucl. Phys. B **18**, 332 (1970)].

[13] A. M. Poskanzer and S. A. Voloshin, Phys. Rev. C **58**, 1671 (1998) [nucl-ex/9805001].

[14] M. Anderson *et al.*, Nucl. Instrum. Meth. A **499**, 659 (2003)

[15] W. J. Llope [STAR Collaboration], Nucl. Instrum. Meth. A **661**, S110 (2012).

[16] C. Adler, A. Denisov, E. Garcia, M. J. Murray, H. Strobele and S. N. White, Nucl. Instrum. Meth. A **470**, 488 (2001); The STAR ZDC-SMD has the same structure as the STAR EEMC SMD: C. E. Allgower et al., Nucl. Instr. Meth. A499, 740 (2003); STAR ZDC-SMD proposal, STAR Note SN-0448 (2003).